Synthesis, Characterization, Structure, Electrochemistry, and Spectroscopy of Porphyrins That Have a Conjugated Connection to Donor/Acceptor Groups

Edia E. Bonfantini, Anthony K. Burrell,* David L. Officer,* and David C. W. Reid

Department of Chemistry, Massey University, Private Bag 11222, Palmerston North, New Zealand

Michael R. McDonald, Paul A. Cocks, and Keith C. Gordon*

Department of Chemistry, University of Otago, P.O. Box 56, Dunedin, New Zealand

Received February 27, 1997[⊗]

The reaction of ((tetraphenylporphyrinyl)methyl)triphenylphosphonium chloride and benzaldehydes ($CHO-C_6H_4-R$; R = H, NO_2, NMe_2, OMe, Me, CHO) yields the styryl porphyrin derivatives. These new styryl-substituted porphyrins have been studied using electrochemistry, electronic absorbance, and resonance Raman spectroelectrochemical techniques. The substituents on the styryl group have a modest perturbation on the electronic spectrum of the porphyrin core. The resonance Raman data suggest that a charge-transfer interaction is observed between the porphyrin core and the NO_2 group for the 4-NO_2 compound.

Introduction

The study of electron transfer to and from porphyrins has been an area of active research for several years. This is largely due to their relationship to the chlorins which play a decisive role in photosynthetic systems.[1] Many model systems have been prepared in an effort to understand the natural photosynthetic systems. As a result the number and variety of synthetic routes toward functionalized porphyrins have expanded rapidly. However, the procedures required to generate functionalized porphyrins generally require either a large number of synthetic steps or rely on the outcome of one or more reactions that produce statistical mixtures. A simple change in the target porphyrin often requires the construction of a completely new synthetic strategy. We have endeavored to develop a synthetic strategy that enables the use of a readily prepared porphyrin that is capable of being simply converted to a wide variety of functional groups. The key to such a system is the use of a single porphyrin starting material in a common reaction with a diverse selection of substrates, to provide a variety of functionalized porphyrins. Toward this end we have been examining substituted porphyrins that are derived from 5,10,15,20-tetraphenylporphyrin (TPP).[2] The result of this investigation has been the preparation of a TPP phosphonium salt derivative **1**, shown in Figure 1.[3] This reagent has provided a general synthetic procedure for the formation of olefin-substituted derivatives of TPP in essentially one step. In this work we report the synthesis of several of these compounds. Of particular interest in these compounds is the effectiveness of the vinyl linker in transferring information to and from the porphyrin core.[4] The level of communication between the porphyrin core and the various aryl groups may be compared by observing the effect of those substituents on the electrochemistry, optical spectroscopy, and Raman spectroscopy of the compounds.

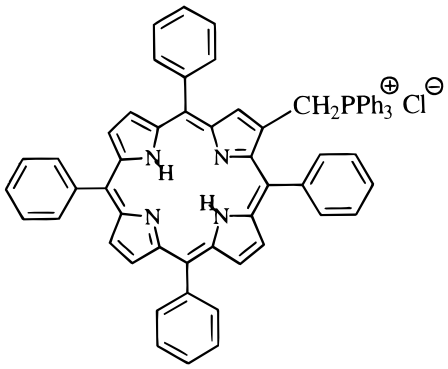

(**1**)

Figure 1. TPP phosphonium salt derivative.

Results

Synthesis. The phosphonium salt **1** is prepared from TPP in five steps in an overall yield of 85%.[3] The reaction of **1** with aryl aldehydes, shown in Scheme 1, can be carried out at room temperature with no special precautions. Thus, the treatment of a solution of **1** and 4-tolualdehyde with base results in the rapid formation of a *cis/trans* mixture of the olefin **3**. It is not necessary to isolate or purify the *cis/trans* mixture because treatment with iodine gives the *trans* isomer exclusively. Simple chromatography then gives **3** in 61% yield. The exclusive

[⊗] Abstract published in *Advance ACS Abstracts,* December 1, 1997.

(1) (a) Deisenhofer, J.; Epp, O.; Miki, K.; Huber, R.; Michel, H. *J. Mol. Biol.* **1984**, *180*, 385. (b) Deisenhofer, J.; Epp, O.; Miki, K.; Huber, R.; Michel, H. *Nature* **1985**, *318*, 618. (c) Chang, C.-H.; Schiffer, M.; Tiede, D.; Smith, U.; Norris, J. *J. Mol. Biol.* **1985**, *186*, 201. (d) Chang, C.-H.; Tiede, D.; Tang, J.; Smith, U.; Norris. J.; Schiffer, M. *FEBS Lett.* **1986**, *205*, 82. (e) Allen, J. P.; Feher, G.; Yeates, T. O.; Rees, D. C.; Deisenhofer, J.; Huber, R. *Proc. Natl. Acad. Sci. U.S.A.* **1986**, *83*, 8589. (f) Allen, J. P.; Feher, G.; Yeates, T. O.; Komiya, H.; Rees, D. C. *Proc. Natl. Acad. Sci. U.S.A.* **1987**, *84*, 5730. (g) Allen, J. P.; Feher, G.; Yeates, T. O.; Komiya, H.; Rees, D. C. *Proc. Natl. Acad. Sci. U.S.A.* **1987**, *84*, 6162. (h) Pearlstein, R. H. *New Compr. Biochem.* **1987**, *15*, 299. (i) Fleming, G. R.; Martin, J.-L.; Breton, J. *Nature* **1988**, *333*, 190.

(2) TPP can be obtained commercially or prepared in large quantities by a simple procedure: Barnett, G. H.; Hudson, M. F.; Smith, K. M. *Tetrahedron Lett.* **1973**, *30*, 2887−2888.

(3) Bonfantini, E. E.; Officer, D. L. *Tetrahedron Lett.* **1993**, *34*, 8531−8534.

(4) Related compounds have been examined in this respect: (a) Wiederrecht, G. P.; Svec, W. A.; Niemczyk, M. P.; Wasielewski, M. R. *J. Phys. Chem.* **1995**, *99*, 8918−8926. (b) Wiederrecht, G. P.; Svec, W. A.; Niemczyk, M. P.; Wasielewski, M. R. *J. Am. Chem. Soc.* **1996**, *118*, 81−88.

S0020-1669(97)00233-4 CCC: $14.00

Scheme 1

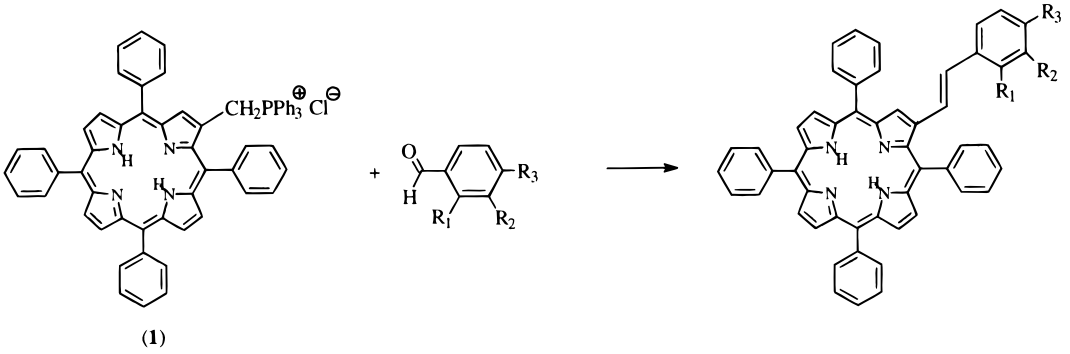

(**1**)

(**2**) R_1 = H, R_2 = H, R_3 = H
(**3**) R_1 = H, R_2 = H, R_3 = CH_3
(**4**) R_1 = H, R_2 = H, R_3 = NO_2
(**5**) R_1 = H, R_2 = NO_2, R_3 = H
(**6**) R_1 = H, R_2 = H, R_3 = CHO
(**7**) R_1 = H, R_2 = CHO, R_3 = H
(**8**) R_1 = CHO, R_2 = H, R_3 = H
(**9**) R_1 = H, R_2 = H, R_3 = OCH_3
(**10**) R_1 = H, R_2 = H, R_3 = $N(CH_3)_2$

presence of the *trans* olefin can be unequivocally determined by ^{1}H NMR spectroscopy. The vinyl protons resonances appear as 16 Hz coupled doublets at 7.30 and 6.96 ppm, respectively. The other notable feature of the ^{1}H NMR spectrum is the signal due to the lone β-pyrrolic proton[5] that appears at 9 ppm as a singlet. This singlet is a general feature that appears in ^{1}H NMR spectra of all of the substituted compounds. Using the same procedure a variety of functionalized porphyrins can be obtained in reasonable yield (Scheme 1). The reaction of **1** with 4-nitrobenzaldehyde proceeds rapidly to give an 81% yield of **4** after purification. Once again the *trans* geometry can be assigned from the presence of two 16 Hz coupled doublets (7.11 and 7.28 ppm) in the ^{1}H NMR spectrum. In general, all of the reactions proceed with reasonable yields although some of the benzaldehydes give lower yields than others; the reactions are apparently influenced by subtle combinations of steric and electronic factors. The lower yields obtained in the formation of the compounds **5** and **10** do not pose a significant problem as the reactions have been successfully scaled-up to give reasonable amounts of product. Thus, the reaction of 614 mg of **1** with isophthalaldehyde yields 343 mg (70%) of **7** after purification. Further modification of these compounds is possible *via* the coordination of metals to the porphyrin core. This is achieved for simple first-row transition metals using standard techniques.[6]

Structure. The presence of the conjugated link between the porphyrin core and the functionalized styrene provides the opportunity for significant communication between these groups. The possibility for there to be communication between the two "ends" of the molecule is strengthened by the geometry observed in the solid-state of **6**·Cu.[7] A single-crystal X-ray diffraction study, shown in Figure 2, of **6**·Cu was carried out, and the porphyrin, olefin, aryl ring, and aldehyde are effectively coplanar. Although the structure in solution may differ from that observed in the solid-state, clearly there is no significant barrier to a planar system. It is also reasonable to assume that all of the 4-substituted derivatives have similar structures to **6**·Cu. Simple modeling using CPK models indicates it is possible for the 2- and the 3-substituted aryl groups to also be coplanar with the porphyrin ring. This raises the question as to how good is the communication between the two parts of the molecule. If the porphyrin and peripheral unit are very strongly coupled, then a large perturbation of the porphyrin properties may be expected. However, the level of coupling may be rather small, resulting in only subtle changes in the porphyrin properties.

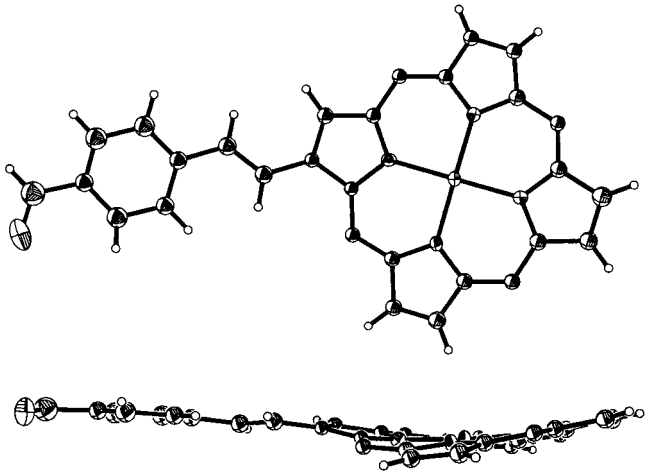

Figure 2. Molecular structure of **6**·Cu with the meso phenyl rings in the lower view omitted for clarity.

Table 1. Electrochemical Data for Porphyrins in CH_2Cl_2

	$E^{o\prime}/V$ [a]			
	oxidation		reduction	
compd				
2	1.03	1.20	−1.16	−1.41
3	1.04	1.21	−1.19	−1.44
4	1.06	1.21	−1.16	−1.41
5	1.05	1.20	−1.14	−1.48
9	1.01	irrev[b]	−1.17	−1.44
10	0.67	irrev	−1.22	−1.53
2·Ni	1.04	1.17	−1.27	−1.61
4·Ni	1.09	1.21	−1.04	−1.21

[a] Versus SCE. [b] Process is irreversible.

Electrochemistry and Spectroscopy. The electrochemical data for the porphyrins are presented in Table 1. Typically the porphyrins show two oxidations and two reductions. It was found that, under the experimental conditions used, the first oxidation and reduction for all systems were reversible.

(5) This signal shows a single weak coupling to one of the olefinic protons in a COSY spectrum.
(6) Falk, J. E. In *Porphyrins and Metalloporphyrins*; Smith, K. M., Ed.; Elsevier: Amsterdam, 1975.
(7) Burrell, A. K.; Officer, D. L.; Reid, D. C. W. *Angew. Chem., Int. Ed. Engl.* **1995**, *34*, 900.

Table 2. Electronic Spectral Data for Porphyrins and Their Oxidized and Reduced Products in CH_2Cl_2 at Room Temperature

compd	λ/nm ($\epsilon \times 10^{-3}$/M^{-1} cm^{-1})				
2	424 (290)	523 (21)	562 (10)	599 (6.5)	655 (2.4)
2^{ox} [a]	445 (127)				667 (14)
2$^-$	420 (140)	518 (sh)	554 (sh)	604 (2.6)	656 (6.8)
3	424 (218)	524 (19)	563 (9.1)	601 (5.7)	655 (6.3)
3^{ox}	447 (82)				667 (8.3)
3$^-$	420 (60)				
4	429 (144)	525 (17)	568 (11)	602 (7.7)	659 (4.5)
4^{ox}					
4$^-$	421 (130)	518 (sh)	553 (sh)	600 (2.4)	656 (3.2)
5	427 (257)	524 (19)	563 (9.1)	600 (6.1)	656 (2.2)
5^{ox}	445 (79)				669 (13)
5$^-$	422 (91)				656 (2.2)
9	422 (151)	524 (9.7)	564 (5.1)	600 (2.7)	657 (1.0)
9^{ox}	447 (193)				667 (22)
9$^-$	419 (102)				
10	421 (166)	521 (16)	572 (7.4)	605 (7.3)	660 (2.0)
10^{ox}	447 (108)				670 (12)
2·Ni	425 (209)	540 (18)	577 (11)		
2·Ni$^+$	418 (43)			604 (9.1)	
4·Ni	431 (189)	541 (17)	583 (14)		
4·Ni$^+$	423 (240)	538 (11)	579 (1.8)		

[a] "ox" indicates oxidized species.

The oxidation potential for **10** is significantly lower than that for the other compounds. This suggests that the NMe_2 group is strongly perturbing the porphyrin ring, stabilizing it toward oxidation, or that the oxidation is centered off the porphyrin and at the NMe_2 functionality. The $E^{\circ\prime}$ for $C_6H_5NMe_2$ lies at 0.65 V vs SCE.[8] Thus, the oxidation potential observed for **10** is close to the potential expected for direct oxidation at the styryl-NMe_2 moiety.

The electronic spectral data for the compounds and their reduced and oxidized products are given in Table 2. The spectrum of **2** is typical of a free-base porphyrin showing a strong B band at about 420 nm and four weaker Q bands to the red of the B transition. The presence of the styryl group in **2** shifts the B band to 424 nm. In H_2TPP the B band lies at 416 nm.[9] The substitution of a methoxy group at the *para* position of the styryl group **9** has no effect on the wavelength of the B band, lying at 422 nm. The *para* substitution of methyl group **3** also has little effect on the wavelength of the B band. However, substitution of a nitro group at *para* **4** or *meta* **5** positions on the styryl group results in a red-shift of the B band to 429 and 427 nm, respectively. Electron donating groups such as NMe_2 result in a blue-shift in the B band to 420 nm. Thus, the substituents on the styryl group have a modest perturbation on the electronic spectrum of the porphyrin core.

The interchelation of nickel into porphyrins **2** and **4** has little effect on the wavelength of the B band. The metal increases the microsymmetry of the ring to D_{4h}. This is borne out by the observation of only two Q bands over the four present for the free-base systems, which have D_{2h} symmetry.[10]

The electronic spectral data of the oxidized products of **2**−**5**, **9**, **10**, **2**·Ni, and **4**·Ni are shown in Table 2. The B band is bleached upon oxidation of **2**·Ni, the new feature growing in is blue-shifted, to 418 nm, and much less intense than the original B band. The two Q bands observed in **2**·Ni are bleached with oxidation, a new band being observed at 604 nm. The changes in the absorption spectrum on going from **4**·Ni to **4**·Ni$^+$ also show a bleach of the Q bands. **4**·Ni$^+$ has a feature at 423 nm, and weak absorbances at 538 and 579 nm. These spectral changes are similar to those reported for the oxidation of TPP·Ni[11] and related complexes.[12]

As the potential is stepped through the oxidation wave, the behavior of the electronic spectra for the free-base systems is interesting. For **2**, oxidation results in a depletion of the B band at 424 nm. A new feature grows in at 445 nm. The four Q bands of **2** are bleached upon oxidation with a new feature appearing at 667 nm with a shoulder at 608 nm. The electronic spectral changes occurring upon oxidation of **3** and **5** and of **9** and **10** are similar to those reported for **2**.

The spectral changes observed for the oxidation of the free-base ligands are unlike those of the nickel(II) complexes. It has been reported that the electrochemical oxidation of H_2TPP readily leads to the formation of other products when attempting to form the monocation.[13] In a series of protonation studies of H_2TPP and related systems, spectral changes almost identical to those observed in this work are reported.[14] The observation of a red-shifted B band and absorption at ca. 655 nm is the spectral signature for the dication species H_4TPP^{2+}.

The monocation of H_2TPP has been observed by photooxidation in low-temperature glasses.[15,16] The spectrum shows vibronic structure in the Q band region. This is absent from our oxidized spectra of free-base porphyrins.

We believe that our spectroelectrochemical experiments are probing the dication rather than monocation species for the free-base systems. To determine this further, the electronic spectra of **3** and **5** were measured in the presence of 2 mole equivalents of trifluoroacetic acid. The spectra observed are identical to those measured in the UV-OTTLE experiment.

The electronic spectral data for species formed by the electrochemical reduction of the porphyrins and nickel complexes are shown in Table 2. The reduction of **3** → **3**$^-$ results in a depletion of the B band. The reduced species absorbs at 420 nm and into the visible region. The intensity of this absorption is much less than that of the neutral species B transition. Porphyrins **2, 4**, **5**, and **9** behave in a very similar fashion to **3** with the B bands bleaching and a new transition appearing to the blue of the B band. The nickel complexes show a depletion of the B band when reduced. For **4**·Ni the radical anion band lies at 419 nm; the species absorbs out to approximately 750 nm.

Resonance Raman spectra (RRS) of the free-base compounds are presented in Figure 3. The resonance Raman signals are very intense from these samples, and the solvent bands are too weak to observe. Table 3 shows the frequencies for all prominent bands in the spectra, which for most of the neutral free-base species are similar. For all of the porphyrins, except **10**, bands lie at 1620, 1550, 1450, 1370, and 1236 cm^{-1}. These common features may be assigned by comparison with the RRS of H_2TPP. Normal coordinate analyses of H_2TPP have been

(8) Meyer, T. J. *Prog. Inorg. Chem.* **1983**, *30*, 389.
(9) Thomas, W.; Martell, A. E. *J. Am. Chem. Soc.* **1956**, *78*, 1338.
(10) Gouterman, M. In *The Porphyrins*; Dolphin, D., Ed.; Academic: London, 1978; Vol. 3, Chapter 1.
(11) Wolberg, A.; Manassen, J. *J. Am. Chem. Soc.* **1970**, *92*, 2982.
(12) Lin, C.-Y.; Hu, S.; Rush, T., III; Spiro, T. G. *J. Am. Chem. Soc.* **1996**, *118*, 9452.
(13) Carnieri, N.; Harriman, A. *Inorg. Chim. Acta*, **1982**, *62*, 103.
(14) Ojadi, C. A.; Linschitz, H.; Gouterman, M.; Walter, R. I.; Lindsey, J. S.; Wagner, R. M.; Droupadi, P. R.; Wang, W. *J. Phys. Chem.* **1993**, *97*, 13192.
(15) Gaysna, Z.; Browett, W. R.; Stillman, M. J. *Inorg. Chim. Acta* **1984**, *92*, 37.
(16) Gaysna, Z.; Browett, W. R.; Stillman, M. J. *Inorg. Chem.* **1985**, *24*, 2440.

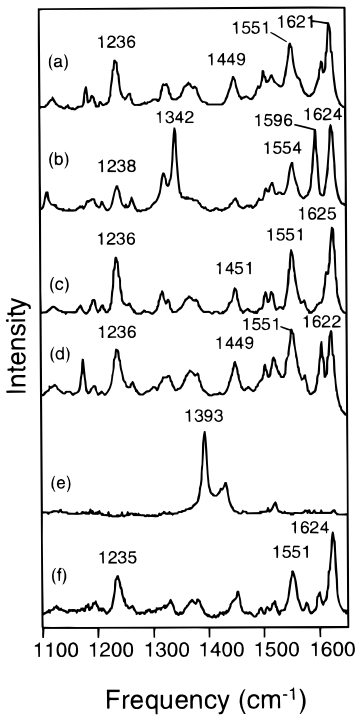

Figure 3. Resonance Raman spectrum of (a) **3**, (b) **4**, (c) **5**, (d) **9**, (e) **10**, and (f) **2** in CH_2Cl_2 (ca. 1 mM), measured with 457.9 nm CW excitation.

published.[17] Using one of these analyses,[17a] the bands at 1607−1596 cm^{-1} are assigned as belonging to the phenyl groups attached at the *meso* carbons. The strong features at ∼1550 cm^{-1} belong to the $C_\beta-C_\beta$ stretch of the porphyrin ring system. This is labeled as ν_2 for H_2TPP. The 1450 cm^{-1} feature is assigned as the porphyrin ring $C_\alpha-C_m$ stretch (labeled as ν_{11} for H_2TPP). The band in the region 1380−1360 cm^{-1} has two possible assignments: It may be the porphyrin symmetric stretch for $C_\alpha-N$, termed ν_4 for H_2TPP, or it may be the asymmetric stretch of the ring system for $C_\alpha-C_\beta$, termed ν_{28}.

In the case of H_2TPP the ν_{28} band is depolarized having B_{1g} symmetry in the D_{2h} point group. The depolarization ratios for the bands observed in the 1380−1360 cm^{-1} region for these porphyrins show that the modes are polarized, hence the possible ν_{28} assignment is discarded. The ν_4 band has A_{1g} symmetry in H_2TPP and is hence polarized. The strong feature at 1236 cm^{-1} in each of the spectra is assigned as the C_m-Ph stretch.

The RRS of the *p*-nitrophenyl derivative **4** and the *p*-(dimethylamino)phenyl compound **10** are significantly different from those of the other porphyrins reported here. First, the C_m-Ph stretch band of **4** at 1238 cm^{-1} is of much lower intensity than for the other spectra. Secondly a very strong feature is observed at 1342 cm^{-1}. This feature is much more intense than the ν_4 band discussed above and is significantly shifted from the anticipated frequency of the ν_4 band. Aromatic species with nitro groups typically show a strong feature at 1340 cm^{-1} ascribed to the nitro group.[18] We assign the feature at 1342 cm^{-1} as that of the nitro group for **4** on the basis of its frequency. It is somewhat surprising that the *meta*-nitro-substituted isomer, **5**, does not show this strong feature. Its spectrum more closely resembles those of **2**, **3**, and **9**. One possible explanation for this is that the nitro group at the *para* position in **4** has a much greater influence over the electronic structure of the porphyrin ring than does the nitro at the *meta* position. In the case of **4**, photoexcitation into the B transition may involve an excited state in which the excited electron is stabilized by the nitro group at the *para* position. Thus the nitro stretch will alter the molecular geometry of the porphyrin in a similar fashion to that of the resonant photoexcitation. This would result in strong enhancement of this mode in the RRS.[19] In the case of **5** the nitro at the *meta* position is less able to perturb the electronic structure of the phenyl group,[20] in terms of stabilizing the excited electron charge, and thus shows weaker resonance enhancement.

The resonance Raman spectrum of the dimethylamino compound **10** (Figure 3e) is also strikingly different from those of the other porphyrins. The strongest feature is at 1393 cm^{-1}; other bands lie at 1430 and 1519 cm^{-1}. Only the 1519 cm^{-1} band is present in the spectra of the other porphyrins. This strong enhancement of non-porphyrin modes may be due to the following. The B transition is strongly perturbed such that the modes enhanced are primarily styryl group vibrations or the substitution of the NMe_2 moiety on the styryl group perturbs the vibrations of the porphyrin core shifting them to new frequencies. The latter explanation may be discounted because the infrared absorbance spectrum of **10** shows a porphyrin signature. It is also possible that photodecomposition of the porphyrin is occurring.

The features observed at 1393 and 1430 cm^{-1} do not correspond well with porphyrin modes. The Raman spectrum of dimethylaminobenzene (DMA) has bands at 1605, 1348, 1195, and 995 cm^{-1} which show moderate to strong intensity. It is possible that these modes would be shifted upon bonding of the DMA unit to the porphyrin.[21]

The free-base porphyrin spectra show some bands that do not correspond to those observed for H_2TPP. Each has a feature at ∼1620 cm^{-1}. We assign this band to the phenyl ring system attached through the double bond to the C_β of the porphyrin ring. Consistent with this assignment, the RRS of 2-methyltetraphenylporphyrin, which has no styryl group, has no feature in this region.

The RRS of the nickel complexes, **4**·Ni (4-nitrophenyl-substituted) and **2**·Ni (phenyl substituted) are shown in Figures 4 and 5, respectively. The spectra differ slightly from those of the corresponding free-base porphyrins. The frequencies of the observed bands (Table 4) may be compared to those of TPP·Ni. A normal coordinate analysis of the Raman spectrum of TPP·Ni has been performed by Li *et al.*[22] Using this analysis the following assignments are made for the strongest features in the Raman spectrum of **2**·Ni: The band at 1600 cm^{-1} is assigned as a phenyl stretch (ϕ_4). The 1570 cm^{-1} band is assigned as the $C_\beta-C_\beta$ stretch (ν_2). The 1377 cm^{-1} is assigned as the pyrrole half-ring symmetric stretch (ν_4). The 1239 cm^{-1} band is assigned as the C_m-Ph stretch (ν_1). These features lie at 1600, 1574, 1373, and 1273 cm^{-1}, respectively, for TPP·Ni. One further band is present at 1624 cm^{-1}. This is assigned as a styryl group vibration because of its similarity in frequency to that for the free-base systems.

The spectrum of **4**·Ni shows the following strong bands which are assigned as TPP·Ni vibrations;[23] 1604 (ϕ_4), 1577 (ν_2), 1376

(17) (a) Stein, P.; Ulman, A.; Spiro, T. G. *J. Phys. Chem.* **1984**, *88*, 369. (b) Bell, S. E. J.; Al-Obaidi, A. H. R.; Hegarty, M. J. N.; McGarvey, J. J.; Hester, R. E. *J. Phys. Chem.* **1995**, *99*, 3959. (c) Li, X.-Y.; Zgierski, M. Z. *J. Phys. Chem.* **1991**, *95*, 4268.
(18) Dollish, F. R.; Fateley, W. G.; Bentley, F. F. In *Characteristic Raman Frequencies of Organic Compounds;* John Wiley & Sons: New York, 1974.
(19) Clark, R. J. H.; Dines, T. J. *Angew. Chem., Int. Ed. Engl.* **1986**, *25*, 131.
(20) Fukui, K.; Yonezawa, T.; Nagata, C.; Shingu, H. *J. Chem. Phys.* **1954**, *22*, 1433.
(21) Brouver, A. M.; Wilbrandt, R. *J. Phys. Chem.*, **1996**, *100*, 9678.
(22) Li, X.-Y.; Czernuszewicz, R. S.; Kincaid, J. R.; Su, Y. O.; Spiro, T. G. *J. Phys. Chem.* **1990**, *94*, 31.

Table 3. Frequencies (cm^{-1}) for Raman Bands of Porphyrins in CH_2Cl_2

H_2TPP[a]	**2**	**3**	**4**	**5**	**9**	**10**	label[a]	assignment[b]
	1624	1621	1624	1625	1622	1626 vw		styryl
1597	1598	1607	1596	1600	1605		ϕ_4	phenyl
1550	1551	1551	1554	1551	1551		ν_2	$\nu(C_\beta-C_\beta)$ pyr-H
	1517	1517	1518	1516	1519	1519 vw		
1499	1505	1503	1505	1504	1503		ν_{12}	$\nu(C_\beta-C_\beta)$ pyr
1438	1450	1449	1450	1451	1449	1430	ν_{11}	$\nu(C_\alpha-C_m)_{sym}$
1383	1380	1380	1379	1380	1381	1393	ν_{28}	$\nu(C_\alpha-C_\beta)_{asym}$
1357	1370	1369	1368	1363	1368		ν_4	ν(pyr half-ring)$_{sym}$
			1342					NO_2
1327	1330	1329		1329	1330			$\delta(N-H)_{in/out\ plane}$
1319		1324	1320	1318	1320			
1292		1305		1287	1302		ν_{12}	ν(pyr half-ring)$_{sym}$ pyr
		1261	1264	1259	1263			
1234	1235	1236	1238	1236	1236		ν_1	$\nu(C_m-Ph)$
1205 sh		1209	1200	1210	1207			

[a] Taken from ref 17a. [b] Assignments taken from refs 17a−c. "sh" denotes shoulder. "vw" denotes peak of very weak intensity.

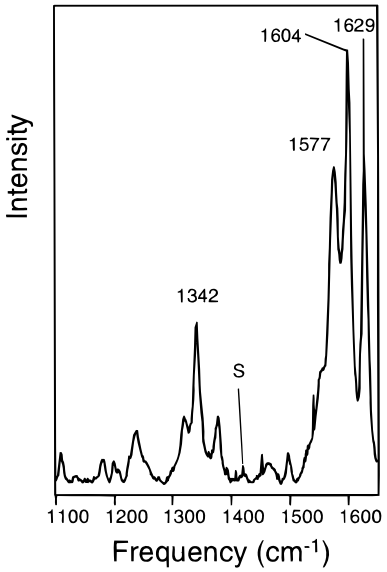

Figure 4. Resonance Raman spectrum of **4**·Ni in CH_2Cl_2 (ca. 1 mM), measured with 457.9 nm CW excitation. S denotes solvent band.

(ν_4), and 1238 (ν_1) cm^{-1}. A styryl vibration is observed at 1629 cm^{-1} and a nitro vibration at 1342 cm^{-1}.

Two features common to the Raman spectra of the oxidized products of **2**−**5** and **9** are strong bands at ca. 1542 and ca. 1385 cm^{-1}.

Complete oxidation of the probed volume is confirmed for each sample by the disappearance of neutral species' bands. For **3** these lie at 1551, 1449, and 1369 cm^{-1}. For **4** bands at 1554 and 1342 cm^{-1} are bleached. For **5** the 1551 and 1363 cm^{-1} bands are lost upon oxidation, for **9** the 1551 and 1449 cm^{-1} bands disappear, and for **2** bands at 1551 and 1450 cm^{-1} are lost. For each system the spectrum observed for the oxidized product has no residual neutral species signal.

The spectra observed in the Raman OTTLE experiment can be reproduced by acidifying the free-base porphyrin with trifluoroacetic acid. Identical bands are observed, confirming that the oxidized free-base systems are dicationic in nature.

The RRS of the oxidized products of the nickel complex **2** is shown in Figure 5. The Raman spectrum of **2**·Ni^+ shows a weaker 1570 cm^{-1} band than in the neutral species. Complete conversion to the oxidized complex is confirmed by the absence of the 1624 cm^{-1} band. The spectrum of the oxidized species shows an intense band at 1363 cm^{-1} and a weaker peak at 1534 cm^{-1}. Attempts to generate the Raman spectrum of **4**·Ni^+ were unsuccessful. The observed spectra were those of the neutral species.

(23) Assignments, as labeled in the preceding reference, are given in parentheses.

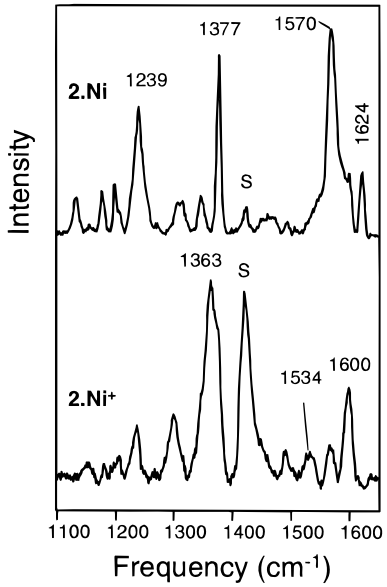

Figure 5. Resonance Raman spectrum of **2**·Ni (lower trace) and **2**·Ni^+ (upper trace) in CH_2Cl_2 (ca. 1 mM), measured with 457.9 nm CW excitation. S denotes solvent band.

Table 4. Frequencies (cm^{-1}) for Raman Bands of Nickel Porphyrins in CH_2Cl_2[a]

2·Ni	**4**·Ni	**2**·Ni	**4**·Ni
1624	1629	1314 w	1319
1600 sh	1604	1306	1238
1570	1577	1239	1207 w
	1546 sh	1200 w	1199 w
	1495 w	1178 w	1179 w
1462 w	1462 w	1133 w	1109 w
1377	1376	1083 w	
1346 w	1342	1010 w	1010 w

[a] "sh" denotes a shoulder. "w" denotes a peak of weak intensity.

Discussion

The similar value of the first oxidation potential for **2**−**5** and **9** with that of H_2TPP suggests that this oxidation is ring based. For metal porphyrins a relationship between the first oxidation (E^{ox}) and first reduction (E^{red}) exists as expounded by Kadish *et al.*[24] For $\delta = 2.20 \pm 0.15$ V (where $\delta = E^{ox} - E^{red}$) it is found that the oxidation is ring, rather than metal, based. The δ for **2**·Ni and **4**·Ni lie in this range.

The optical absorption spectra of the porphyrins offer some insight into the level of perturbation of the porphyrin chromophore by the styryl groups. The electronic spectra of the porphyrin chromophores arise through transitions from the HOMOs of a_{1u} and a_{2u} symmetry to the e_g LUMOs from the four orbital model.[25] The most important factor in determining the wavelengths and oscillator strengths for the B and Q transitions is the configuration interaction between the a_{1u} and a_{2u} orbitals.[25] The effects of substituents upon the energies of the highest occupied orbitals may be predicted, but the relationship between orbital energy and transition wavelength is not straightforward. Because the four-orbital model has been calculated for a D_{4h} point group, it is applicable to the nickel complexes in this study. Shelnutt's[26] analysis of the transition energies of B and Q bands (E_B and E_Q, respectively) to the square of the dipole strengths for these transitions (q_B^2 and q_Q^2, respectively) reveals that the closer in energy the a_{1u} and a_{2u} orbitals are the smaller q_B^2/q_Q^2 and the smaller $E_B - E_Q$ are. The $E_B - E_Q$ values are 6430, 6130, and 6050 cm^{-1} for TPP·Ni, **2**·Ni, and **4**·Ni, respectively. The q_B^2/q_Q^2 values are 0,[26] 0.028, and 0.053, respectively.[27] The bandwidth of the B band for **4**·Ni is considerably greater than that of **2**·Ni (2500 and 1700 cm^{-1}, respectively). These values imply that the energies of the a_{1u} and a_{2u} orbitals are further apart in these systems than in TPP complexes.

The poor correlation between the oscillator strengths and transition energies may be caused by the very small data set used or the presence of the styryl group which may modify the orbitals involved because of symmetry reduction. It may also be due to the presence of the nitro group. This may result in one or both of the transitions having charge-transfer character. Spectra of amino-substituted porphyrins show a marked increase in B transition bandwidth which has been attributed to increased CT character in the transition.[28]

The most likely explanation for the poor correlation is the small size of the data set. Furthermore, this illustrates the difficulty in analyzing the optical spectra of these porphyrins.

The changes in the electronic spectra upon oxidation are interesting. For the nickel complexes, the oxidation results in a blue-shift of the B-band. This is typical of oxidized metalloporphyrins in which the oxidation occurs at the porphyrin ring.[28] Unfortunately the blue-shift of the absorption and its diminished intensity reduce the resonance effect at the available excitation wavelength. Thus the RRS of the oxidized nickel complexes are weaker than the neutral species. For **4**·Ni^+ no appreciable signal is observed.

Insertion of the nickel into the porphyrin ring has a number of effects relative to the free-base porphyrins; the frequency of some bands and the energy of the Q bands increase.[29]

The ν_2 band in **2**·Ni lies at 1570 cm^{-1}, 19 cm^{-1} higher than the ν_2 band for **2**. The ν_4 band lies at 1377 cm^{-1}, 7 cm^{-1} higher than **2**. The C_m−Ph mode is 4 cm^{-1} higher, and the ϕ_4 is 2 cm^{-1} higher. The values for E_Q are 17.3×10^3 and 16.8×10^3 cm^{-1} for **2**·Ni and **2**, respectively.

The value of E_Q is related to the electronegativity of the metal center for metalloporphyrins.[25] In a study of the Raman and electronic spectroscopy of OEP·Ni (OEP is octaethylporphyrin), Kitigawa[30] noted a correlation between the modes discussed above and the E_Q values. The metal center perturbs the energy of the a_{2u} orbital because of the high wavefunction amplitude of a_{2u} on the nitrogen atoms of the porphyrin. The a_{1u} orbital has negligible amplitude at the nitrogens. The presence of a metal results in stabilization of the a_{2u} orbital which causes the MO to become more bonding, thereby increasing bond order of the porphyrin ring. The increased bond order results in an increase in vibrational frequency for the porphyrin modes.

This explanation appears appropriate for **2** and **2**·Ni. A stabilization of the a_{2u} MO would have little affect on the bond order within the phenyl groups appended at the *meso* carbon or the C_m−ϕ bond. Consistent with this there is little shift in the ϕ_4 or C_m−Ph vibrational frequencies. However, for the C_β−C_β stretch (ν_2) the a_{2u} orbital is bonding therefore a more substantial frequency increase would be predicted for this mode. This is indeed observed. The ν_4 band involves the extension of the C_α−N linkage concomitant with the compression of the C_α−C_β bond and motion of the N toward the metal center. For the a_{2u} orbital, the C_α−C_β bond is weakly antibonding, the C_α−N more strongly antibonding, and the N−metal strongly bonding. This last interaction appears to be the most important as the ν_4 band shifts up in frequency with nickel insertion. A very similar correlation exists for **4** and **4**·Ni. The E_Q values are 16.4×10^3 and 17.1×10^3 cm^{-1}, respectively. The shifts with nickel insertion are +8, +23, +8, and 0 cm^{-1} for the ϕ_4, ν_2, ν_4, and ν_1 modes, respectively.[23]

The highest occupied energy MOs in a porphyrin system are those with a_{1u} and a_{2u} symmetry. The spectral features observed upon oxidation will depend on which of these MOs is depopulated. This can be determined from analysis of the resonance Raman spectral changes upon oxidation of the species. The resonance Raman spectra of the porphyrins and their radical cations are well understood,[31] and the shift patterns on going from neutral to oxidized species provide evidence as to the nature of the MO depopulated. In the spectra of **2**·Ni, the most notable shifts occur from 1570 → 1534 cm^{-1} (ν_2 C_β−C_β stretch) and from 1377 → 1363 cm^{-1} (ν_4). Similar shifts are observed in the spectra of TPP·Cu and TPP·Cu^+. The shift of the ν_2 band is particularly useful because the a_{1u} MO is antibonding with respect to the C_β−C_β linkage whereas the a_{2u} MO is bonding over C_β−C_β. The observation of the frequency downshift in the ν_2 band indicates that the electron has been taken from an MO of a_{2u} symmetry.

Conclusions

The reactions of **1** with aryl aldehydes represents a simple high yielding method for functionalizing porphyrins. The reaction is tolerant of a range of functional groups on the aldehyde. Thus compounds with both electron-withdrawing (NO_2) and electron-donating (NMe_2) groups are readily prepared. X-ray structural data indicate that the porphyrin core and the styryl groups are coplanar.

The perturbation of the porphyrin core by the substituted styryl substituents is rather more subtle than that observed for other porphyrin systems, which are linked by bridging units. For the substitutents used here only modest changes in electronic spectra and electrochemistry are seen. Furthermore the Q bands behave as they would in D_{2h} (for free-base systems) and D_{4h} (metal complexes) symmetry environments. This is consistent

(24) Fuhrhop, J.-H.; Kadish, K. M.; Davis, D. G. *J. Am. Chem. Soc.* **1973**, *95*, 5140.
(25) Gouterman, M. *J. Chem. Phys.* **1959**, *30* 1139.
(26) (a) Shelnutt, J. A. *J. Phys. Chem.* **1984**, *88*, 4988. (b) Shelnutt, J. A.; Ortiz, V. *J. Phys. Chem.* **1985**, *89*, 4733.
(27) The value of q_B^2/q_Q^2 was taken from ref 26. $q^2 \sim f/E$ where f is the oscillator strength. $f \sim \epsilon_{max}\Delta\nu$, where ϵ_{max} is the maximum extinction coefficient value and $\Delta\nu$ is the bandwidth of the transition in cm^{-1}. The error in q_B^2/q_Q^2 would be ± 10%.
(28) Fuhrhop, J.-H. *Struct. Bond.* **1974**, *18*, 1.
(29) E_Q for the free-base is calculated as the average energy for the two 0−0 transitions.
(30) Kitagawa, T. *J. Phys. Chem.* **1975**, *79*, 2629.
(31) Czernuszewicz, R. S.; Macor, K. A.; Li, X.-Y.; Kincaid, J. R.; Spiro, T. G. *J. Am. Chem. Soc.* **1989**, *111*, 3860.

with the substituents having a very small effect on the porphyrin core. However, the substituents do have a subtle effect which suggests the styryl group and porphyrin ring are coplanar. This is evidenced by the enhancement of the styryl vibrations in the resonance Raman spectra and by the nitro vibration in **4** and **4**·Ni. The increase in bandwidth for the B-band also suggests a charge-transfer interaction from the electron-withdrawing nitro moiety to the porphyrin.

It would appear that substituents on the C_β position linked by a double bond are planar but do not strongly perturb the porphyrin. This offers the interesting possibility of creating an array of porphyrins which maintain the individual chromophoric and redox properties of the monomer porphyrin while allowing interactions between the porphyrin components of the array.

Experimental Procedures

For electrochemical and spectroscopic measurements spectroscopic grade CH_2Cl_2 was used. The supporting electrolyte used in the electrochemical measurements was tetrabutylammonium perchlorate (TBAP). This was purified by repeated recrystallizations from ethanol/water.[32]

Physical Measurements. A Perkin-Elmer λ-19 spectrometer was used for collection of electronic absorption spectra. Extinction coefficients were obtained from a least squares analysis of a series of solutions at different concentrations.

Cyclic voltammograms (CVs) were obtained from degassed solutions of compound (*ca.* 1 mM) with 0.1 M concentration of TBAP present. The electrochemical cell consisted of a 1.6 mm diameter platinum working electrode embedded in a Kel-F cylinder with a platinum auxiliary electrode and a saturated potassium chloride calomel reference electrode. The potential of the cell was controlled by an EG&G PAR 273A potentiostat with model 270 software.

Raman scattering was generated using a Spectra-Physics model 166 argon ion laser with an excitation wavelength of 457.9 nm. Raman spectra were collected in a backscattering geometry with a two lens arrangement.[33] The irradiated volume was imaged into a Spex 750M spectrograph equipped with an 1800 groove/mm holographic grating. A Princeton Instruments 1152-EUV CCD was used for photon detection. A 150 μm entrance slit was used; with 457.9 nm excitation, this provided a resolution of approximately 5 cm^{-1} for the Raman spectra reported.

Raman spectra were calibrated using emission lines from the argon ion excitation source or a neon lamp. The calibrations were checked against a known solvent spectrum; peak frequency reproducibility was found to be good to 1 cm^{-1}.[34]

Spectroelectrochemical measurements (Raman and electronic absorption) were made using an optically transparent thin-layer electrochemical (OTTLE) cell.[35] For the electronic absorption measurements the cell was set to a potential for 10 min and then the spectrum recorded. Spectra were measured at a series of potentials spanning the reduction or oxidation. For the Raman measurements the potential was set past the $E^{\circ\prime}$ for the oxidation or reduction of interest. Measurements were made only at this potential.

^{1}H nuclear magnetic resonance spectra were obtained at 270 MHz using a JEOL GX270 spectrometer. ^{1}H nuclear magnetic resonance data are expressed in ppm downfield shift from tetramethylsilane as an internal reference and are reported as position (δ_H), relative integral, multiplicity (s = singlet, d = doublet, dd = double of doublet, ddd = double double doublet, t = triplet, q = quartet, and m = multiplet), coupling constant (*J*, Hz) and assignment. Flash chromatography used Merck Kieselgel 60 (230−400 mesh) with the indicated solvents. Thin-layer chromatography was performed using precoated silica gel plates (Merck Kieselgel 60F_{254}). The syntheses of **1**[3] and **6**[7] have been reported previously.

(*trans*-2-(5,10,15,20-Tetraphenylporphyrin-2-yl)ethen-1-yl)benzene (2). To a solution of phosphonium salt **1** (75 mg, 81 μmol) and benzaldehyde (25 mg, 0.24 mmol) in CH_2Cl_2 (0.4 mL) was added a 45% aqueous NaOH solution (0.3 mL). After stirring for 1 h at room temperature, water (30 mL) was added and the mixture extracted twice with CH_2Cl_2 (30 mL, 20 mL). The combined organic phases were washed with water (50 mL) and dried ($MgSO_4$). The solvent was removed, and the residue was purified by flash column chromatography (silica, 1:1 CH_2Cl_2/hexane). The resulting material was recrystallized from CH_2Cl_2/MeOH, to give **2** (51 mg, 88%) as a purple solid. ^{1}H-NMR (270 MHz, $CDCl_3$): δ −2.61 (br s, 2H, NH), 6.99 (d, 1H, ^3J = 15.9 Hz, $H_{ethenyl}$), 7.26−7.37 (m, 6H, H_{Ar} and $H_{ethenyl}$), 7.70−7.83 (m, 12H, $H_{m,pPh}$), 8.17−8.26 (m, 8H, H_{oPh}), 8.71−8.83 (m, 6H, $H_{pyrrole}$), 9.00 (s, 1H, $H_{pyrrole}$). UV−vis (CH_2Cl_2): λ_{max} (log ϵ) 424 (5.46), 523 (4.32), 562 (4.00), 599 (3.81), 655 (3.38) nm. HRMS, *m*/*z*: calcd for MH^+ ($C_{52}H_{37}N_4$), 717.3018; found, 717.3023.

4-(*trans*-2-(5,10,15,20-Tetraphenylporphyrin-2-yl)ethen-1-yl))-toluene (3). Phosphonium salt **1** (100 mg, 0.108 mmol) and tolualdehyde (14 μL, 14.2 mg, 0.119 mmol) were dissolved in CH_2Cl_2 (4 mL) and stirred at room temperature before adding DBU (100 μL, 0.669 mmol). After 5 min, the reaction mixture was flash column chromatographed (silica, 1:2 CH_2Cl_2/hexane) to give a *cis*/*trans* (∼1:3 by ^{1}H NMR) mixture of products. The material was dissolved in CH_2Cl_2 (10 mL), and I_2 (8.5 mg, 33 μmol) was added before stirring at room temperature for 16 h. The reaction was diluted with CH_2Cl_2 (20 mL) and washed with 1 M aqueous $Na_2S_2O_3$ (2 × 20 mL) and H_2O (2 × 20 mL), dried ($MgSO_4$), and the solvent was removed under reduced pressure. Flash chromatography (silica, 1:1 CH_2Cl_2/hexane) followed by recrystallization from CH_2Cl_2/CH_3OH, yielded **3** (48 mg, 61%) as a purple solid. ^{1}H-NMR (270 MHz, $CDCl_3$): δ −2.59 (br s, 2H, NH), 2.41 (s, 3H, H_{Me}), 6.96 (d, 1H, ^3J = 16.0 Hz, $H_{ethenyl}$), 7.17 (s, 4H, H_{Ar}), 7.30 (d, 1H, ^3J = 16.0 Hz, $H_{ethenyl}$), 7.72−7.85 (m, 12H, $H_{m,pPh}$), 8.19−8.29 (m, 8H, H_{oPh}), 8.71−8.87 (m, 6H, $H_{pyrrole}$), 9.01 (s, 1H, $H_{pyrrole}$). UV−vis (CH_2Cl_2) λ_{max} (log ϵ) 424 (5.37), 524 (4.32), 563 (4.09), 601 (3.88), 655 (3.41) nm. HRMS, *m*/*z*: calcd for MH^+ ($C_{53}H_{39}N_4$), 731.3175; found, 731.3189.

4-(*trans*-2-(5,10,15,20-Tetraphenylporphyrin-2-yl)ethen-1-yl)nitrobenzene (4). To a solution of phosphonium salt **1** (66 mg, 71 μmol) and 4-nitrobenzaldehyde (18 mg, 0.12 mmol) in CH_2Cl_2 (0.5 mL) was added aqueous 25% NaOH solution (0.5 mL). After being stirred for 30 min, the mixture was diluted with CH_2Cl_2 (3 mL) and stirred for an additional 10 min. Water was added, and the mixture was extracted with CH_2Cl_2 (40 mL, 30 mL). The combined organic phases were washed with water (2 × 40 mL) and dried ($MgSO_4$). The solvent was removed *in vacuo*, and the residue purified by flash column chromatography (silica, 3:2 CH_2Cl_2/hexane). The major band gave a mixture of *cis*/*trans* isomers (1:3 by ^{1}H NMR). This mixture was stirred with I_2 (20 mg, 79 μmol) in CH_2Cl_2 (3 mL) for 24 h, diluted with CH_2Cl_2, and washed with 15% aqueous $Na_2S_2O_3$ (2 × 20 mL) and then water (2 × 20 mL). After drying ($MgSO_4$), solvent removal *in vacuo*, and recrystallization from CH_2Cl_2/MeOH, **4** (44 mg, 81%) was obtained. ^{1}H-NMR (270 MHz, $CDCl_3$): δ −2.60 (br s, 2H, NH), 7.11 (d, 1H, ^3J = 16.0 Hz, $H_{ethenyl}$), 7.28 (d, 1H, ^3J = 16.0 Hz, $H_{ethenyl}$), 7.30 (d, 2H, ^3J = 8.6 Hz, H_{Ar}), 7.71−7.83 (m, 12H, $H_{m,pPh}$), 8.14−8.26 (m, 10H, H_oPh and H_{Ar}), 8.72−8.84 (m, 6H, $H_{pyrrole}$), 9.02 (s, 1H, $H_{pyrrole}$). UV−vis (CH_2Cl_2): λ_{max} (log ϵ) 429 (5.16), 525 (4.23) 568 (4.04), 602 (3.89), 659 (3.65) nm. HRMS, *m*/*z*: calcd for MH^+ ($C_{52}H_{36}N_5O_2$), 762.2869; found, 762.2891.

3-(*trans*-2-(5,10,15,20-Tetraphenylporphyrin-2-yl)ethen-1-yl)nitrobenzene (5). Phosphonium salt **1** (202 mg, 0.218 mmol) and 3-nitrobenzaldehyde (34 mg, 0.22 mmol) were dissolved in CH_2Cl_2 (4 mL) and stirred at room temperature before addition of DBU (0.2 mL, 1.34 mmol). After 1 h, the reaction mixture was flash column chromatographed (silica, 1:1 CH_2Cl_2/hexane) to give a *cis*/*trans* (3:5 by ^{1}H NMR) mixture of products as a purple solid. The solid was dissolved in CH_2Cl_2 (20 mL), and I_2 (15 mg, 59 μmol) was added before stirring at room temperature for 16 h. The reaction was diluted with CH_2Cl_2 (20 mL), washed with 1 M aqueous $Na_2S_2O_3$ (2 × 40 mL) and H_2O (2 × 20 mL), dried ($MgSO_4$) and solvent removed under reduced pressure. Flash chromatography as before followed by recrystallization from CH_2Cl_2/CH_3OH yielded **5** (73 mg, 44%) as a purple solid. ^{1}H-NMR (270 MHz, $CDCl_3$): δ −2.58 (br s, 2H, NH), 7.07 (d, 1H, ^3J =

(32) House, H. O.; Feng, E.; Peet, N. P. *J. Org. Chem.* **1971**, *36*, 2371.
(33) Strommen, D. P.; Nakamoto, K. *Laboratory Raman Spectroscopy*; John Wiley & Sons Inc.: New York, 1984.
(34) Ferraro, J. R.; Nakamoto, K. *Introductory Raman Spectroscopy*; Academic Press Inc.: San Diego, CA, 1994.
(35) McQuillan, A. J.; Babaei, A. *J. Chem. Educ.*, in press.

16.2 Hz, $H_{ethenyl}$), 7.31 (d, 1H, ^3J = 16.2 Hz, $H_{ethenyl}$), 7.43−7.58 (m, 2H, H_{Ar}), 7.74−7.96 (m, 12H, $H_{m,pPh}$), 8.05−8.12 (m, 2H, H_{Ar}), 8.20−8.29 (m, 8H, H_{oPh}), 8.77−8.86 (m, 6H, $H_{pyrrole}$), 9.04 (s, 1H, $H_{pyrrole}$). UV−vis (CH_2Cl_2): λ_{max} (log ϵ) 427 (5.36), 524 (4.29), 563 (3.99), 600 (3.82), 656 (3.40) nm. HRMS, *m*/*z*: calcd for MH^+ ($C_{52}H_{36}N_5O_2$), 762.2869; found, 762.2861.

3-(*trans*-2-(5,10,15,20-Tetraphenylporphyrin-2-yl)ethen-1-yl)-benzaldehyde (7). To a solution of phosphonium salt **1** (614 mg, 0.663 mmol) and isophthalaldehyde (89 mg, 0.66 mmol) in CH_2Cl_2 (6 mL), was added a 28% aqueous NaOH solution (8 mL). After 3 h of stirring at room temperature, water (50 mL) was added and the mixture extracted with CH_2Cl_2 (2 × 50 mL). The combined organic phases were washed with water (2 × 50 mL) and dried ($MgSO_4$) before the solvent was removed under reduced pressure. The residue was purified by flash column chromatography (silica, 2:1 CH_2Cl_2/hexane) to give a *cis*/*trans* (∼1:2 by ^{1}H NMR) mixture of products as a purple solid. The solid was dissolved in CH_2Cl_2 (100 mL) and I_2 (35 mg, 0.14 mmol) added. After stirring at room temperature in the dark for 16 h, the reaction mixture was washed with 1 M $Na_2S_2O_3$ (2 × 50 mL), water (50 mL), and saturated aqueous $NaHCO_3$ (50 mL). The porphyrin solution was dried ($MgSO_4$), and solvent was removed under reduced pressure. Flash chromatography as before and recrystallization from CH_2Cl_2/MeOH yielded **7** (343 mg, 70%) as a purple solid. ^{1}H-NMR (270 MHz, $CDCl_3$), δ −2.59 (br s, 2H, NH), 7.05 (d, 1H, ^3J = 16.0 Hz, $H_{ethenyl}$), 7.30 (d, 1H, ^3J = 16.0 Hz, $H_{ethenyl}$), 7.42−7.47 (m, 2H, H_{Ar}), 7.67−7.85 (m, 14H, $H_{m,pPh}$ and H_{Ar}), 8.15−8.27 (m, 8H, H_{oPh}), 8.71−8.84 (m, 6H, $H_{pyrrole}$), 9.01 (s, 1H, $H_{pyrrole}$), 10.05 (s, 1H, CHO). UV−vis (CH_2Cl_2): λ_{max} (log ϵ) 426 (5.37), 524 (4.30), 563 (4.03), 599 (3.85), 656 (3.41) nm. HRMS, *m*/*z*: calcd for MH^+ ($C_{53}H_{37}N_4O$), 745.2967; found, 745.3028.

2-(*trans*-2-5,10,15,20-Tetraphenylporphyrin-2-yl))ethen-1-yl)-benzaldehyde (8). To a solution of phosphonium salt **1** (416 mg, 0.449 mmol) and phthalaldehyde (61 mg, 0.455 mmol) in CH_2Cl_2 (6 mL) was added a 40% aqueous NaOH solution (6 mL). After being stirred for 10 min at room temperature, water (50 mL) was added and the mixture was extracted with CH_2Cl_2 (100 mL). The extract was washed with water (2 × 50 mL) and dried ($MgSO_4$) before the solvent was removed under reduced pressure. The residue was purified by flash column chromatography (silica gel, 2:1 CH_2Cl_2/hexane) to give a *cis*/*trans* (∼1:3 by ^{1}H-NMR) mixture of products as a purple solid. The solid was dissolved in CH_2Cl_2 (100 mL) and I_2 (30 mg, 0.12 mmol) added. After stirring at room temperature in the dark for 16 h, the reaction mixture was washed with 1 M $Na_2S_2O_3$ (2 × 50 mL), water (50 mL), and saturated aqueous $NaHCO_3$ (50 mL). The porphyrin solution was dried ($MgSO_4$), and solvent was removed under reduced pressure. Flash chromatography as before and recrystallization from CH_2Cl_2/MeOH yielded **8** (263 mg, 79%) as a purple powder. ^{1}H-NMR (270 MHz, $CDCl_3$): δ −2.59 (br s, 2H, NH), 6.96 (d, 1H, ^3J = 15.9 Hz, $H_{ethenyl}$), 7.19 (d, 1H, ^3J = 7.3 Hz, H_{Ar}), 7.34 (app t, 1H, ^3J = 7.3 Hz, H_{Ar}), 7.52 (app t of d, 1H, ^3J = 7.3 Hz, ^4J = 1.2 Hz, H_{Ar}), 7.65−7.80 (m, 13H, $H_{m,pPh}$ and H_{Ar}), 8.13−8.27 (m, 9H, H_{oPh} and $H_{ethenyl}$), 8.69 (d, 1H, ^3J = 4.9 Hz, $H_{pyrrole}$), 8.78 (d, 1H, ^3J = 4.9 Hz, $H_{pyrrole}$), 8.80−8.86 (m, 4 H, $H_{pyrrole}$), 9.06 (s, 1H, $H_{pyrrole}$), 10.37 (s, 1H, CHO). UV−vis (CH_2Cl_2), λ_{max} (log ϵ) 427 (5.51), 523 (4.44), 564 (4.16), 600 (3.99), 657 (3.59) nm. HRMS, *m*/*z*: calcd for M^+ ($C_{53}H_{36}N_4O$), 744.2889; found, 744.2908.

4-(*trans*-2-(5,10,15,20-Tetraphenylporphyrin-2-yl)ethen-1-yl)anisole (9). Phosphonium salt **1** (80 mg, 86 μmol) and anisaldehyde (15 mg, 0.110 mmol) were dissolved in CH_2Cl_2 (5 mL), and the solution was stirred at room temperature before adding DBU (80 μL, 0.535 mmol). After 10 min, the reaction mixture was flash column chromatographed (silica, 1:1 CH_2Cl_2/hexane) to give a *cis*/*trans* mixture (∼1:4 by ^{1}H NMR) of products as a purple solid. The solid was dissolved in CH_2Cl_2 (10 mL) and I_2 (8.5 mg, 33 μmol) added before stirring at room temperature for 16 h. The reaction was diluted with CH_2Cl_2 (20 mL), washed with 1 M aqueous $Na_2S_2O_3$ (2 × 20 mL) and H_2O (2 × 20 mL), and dried ($MgSO_4$), and solvent was removed under reduced pressure. Flash column chromatography as before, followed by recrystallization from CH_2Cl_2/CH_3OH, yielded **9** (40 mg, 62%) as a purple solid. ^{1}H-NMR (270 MHz, $CDCl_3$): δ −2.55 (br s, 2H, NH), 3.89 (s, 3H, H_{OMe}), 6.89 (d, 1H, ^3J = 16.0 Hz, $H_{ethenyl}$), 6.92 (d, 2H, ^3J = 8.7 Hz, H_{Ar}), 7.25 (d, 2H, ^3J = 8.7 Hz, H_{Ar}), 7.32 (d, 1H, ^3J = 16.0 Hz, $H_{ethenyl}$), 7.74−7.89 (m, 12H, $H_{m,pPh}$), 8.22−8.34 (m, 8H, H_{oPh}), 8.75−8.95 (m, 6H, $H_{pyrrole}$), 9.05 (s, 1H, $H_{pyrrole}$). UV−vis (CH_2Cl_2): λ_{max} (log ϵ) 422 (5.18), 524 (3.99), 564 (3.71), 600 (3.43), 657 (3.00) nm. HRMS, *m*/*z*: calcd for M^+ ($C_{53}H_{38}N_4O$), 746.3046; found, 746.3025.

4-(*trans*-2-(5,10,15,20-Tetraphenylporphyrin-2-yl)ethen-1-yl)-*N*,*N*-dimethylaniline (10). To a solution of phosphonium salt **1** (90 mg, 97 μmol) and 4-(dimethylamino)benzaldehyde (23 mg, 154 μmol) in CH_2Cl_2 (0.6 mL) was added an aqueous 40% NaOH solution (0.6 mL). The mixture was stirred for 105 min and then poured into water (50 mL) and extracted with CH_2Cl_2 (50 mL, 30 mL). The combined organic extracts were washed with water (2 × 50 mL) and dried ($MgSO_4$). The solvent was removed *in vacuo*, and the residue was purified by flash column chromatography (silica, 1:1 CH_2Cl_2/hexane). The resulting material was recrystallized from CH_2Cl_2/MeOH, affording **10** (48 mg, 65%) as a purple solid. ^{1}H-NMR (270 MHz, $CDCl_3$): δ −2.56 (br s, 2H, NH), 6.70 (d, 2H, ^3J = 8.9 Hz, H_{Ar}), 6.77 (d, 1H, ^3J = 16.2 Hz, $H_{ethenyl}$), 7.16 (d, 2H, ^3J = 8.9 Hz, H_{Ar}), 7.27 (d, 1H, ^3J = 15.9 Hz, $H_{ethenyl}$), 7.71−7.83 (m, 12H, $H_{m,pPh}$), 8.14−8.26 (m, 8H, H_{oPh}), 8.72−8.84 (m, 6H, $H_{pyrrole}$), 9.02 (s, 1H, $H_{pyrrole}$). UV−vis (CH_2Cl_2): λ_{max} (log ϵ) 421 (5.22), 521 (4.20), 572 (3.87), 605 (3.86), 660 (3.30) nm. HRMS, *m*/*z*: calcd for MH^+ ($C_{54}H_{42}N_5$), 760.3440; found, 760.3419.

2·Ni. Free-base porphyrin **2** (40 mg, 56 μmol) was refluxed in $CHCl_3$ (4 mL) and a slurry of $Ni(OAc)_2$·$4H_2O$ (117 mg, 0.47 mmol) in CH_3OH/H_2O (1 mL/0.2 mL) added. Triethylamine (3 drops) was added, and refluxing continued for 16 h. After cooling, the reaction mixture was diluted with CH_2Cl_2 (20 mL) and washed with water (20 mL) and saturated aqueous $NaHCO_3$ (20 mL). Drying ($MgSO_4$) and removal of solvent under reduced pressure gave a purple solid. Flash column chromatography (silica, CH_2Cl_2/cyclohexane 1:2) followed by recrystallization from CH_2Cl_2/CH_3OH, gave **2**·Ni (26 mg, 60%) as a red-purple solid as well as recovered starting material (12 mg, 30%). ^{1}H-NMR (270 MHz, $CDCl_3$): δ 6.87 (d, 1H, ^3J = 16.0 Hz, $H_{ethenyl}$), 7.18−7.34 (m, 5H, H_{Ar}), 7.14 (d, 1H, ^3J = 16.0 Hz, $H_{ethenyl}$), 7.65−7.76 (m, 12H, $H_{m,pPh}$), 7.97−8.07 (m, 8H, H_{oPh}), 8.69−8.73 (m, 6H, $H_{pyrrole}$), 8.90 (s, 1H, $H_{pyrrole}$). UV−vis (CH_2Cl_2): λ_{max} (log ϵ) 425 (5.32), 540 (4.26), 577 (4.04) nm. HRMS, *m*/*z*: calcd for M^+ ($C_{52}H_{34}N_4{}^{58}Ni$), 772.2137; found, 772.2132.

4·Ni. Nitrobenzene (**4**) (28 mg, 37 μmol) was refluxed in $CHCl_3$ (30 mL) and a slurry of $Ni(OAc)_2$·$4H_2O$ (102 mg, 0.41 mmol) in CH_3OH/H_2O (1 mL/0.2 mL) added. The mixture was refluxed for 16 h, cooled, washed with water (20 mL), and dried ($MgSO_4$), and solvent was removed under reduced pressure. Recrystallization from CH_2Cl_2/CH_3OH gave **4**·Ni (30 mg, quantitative) as a red-purple solid. ^{1}H-NMR (270 MHz, $CDCl_3$): δ 6.92 (d, 1H, ^3J = 15.9 Hz, $H_{ethenyl}$), 7.06 (d, 1H, ^3J = 15.9 Hz, $H_{ethenyl}$), 7.14 (d, 2H, ^3J = 8.5 Hz, H_{Ar}), 7.58−7.73 (m, 12H, $H_{m,pPh}$), 7.90−8.03 (m, 8H, H_{oPh}), 8.05 (d, 2H, ^3J = 8.6 Hz, H_{Ar}), 8.63−8.72 (m, 6H, $H_{pyrrole}$), 8.89 (s, 1H, $H_{pyrrole}$). UV−vis (CH_2Cl_2): λ_{max} (log ϵ) 431 (5.28), 541 (4.23), 583 (4.15) nm. HRMS, *m*/*z*: calcd for MH^+ ($C_{52}H_{34}N_5O_2{}^{58}Ni$), 818.2066; found, 818.2096.

6·Cu. Aldehyde **6** (31 mg, 42 μmol) was refluxed in $CHCl_3$ (8 mL), and a slurry of $Cu(OAc)_2$·H_2O (97 mg, 0.49 mmol) in CH_3OH/H_2O (0.5 mL/0.1 mL) was added. Refluxing was continued for 90 min. The reaction mixture was diluted with CH_2Cl_2 (20 mL), washed with water (20 mL), and dried ($MgSO_4$), and solvent was removed under reduced pressure. Flash column chromatography (silica, 2:1 CH_2Cl_2/hexane) followed by recrystallization from CH_2Cl_2/CH_3OH gave **6**·Cu (29 mg, 86%) as a red-purple solid. UV−vis (CH_2Cl_2): λ_{max} (log ϵ) 428 (5.35), 549 (4.36), 587 (4.13) nm. HRMS, *m*/*z*: calcd for MH^+ ($C_{53}H_{35}N_4O^{63}Cu$), 806.2107; found, 806.2091.

6·Ni. Aldehyde **6** (33 mg, 44 μmol) was heated at reflux temperature in $CHCl_3$ (10 mL) and a slurry of $Ni(OAc)_2$·$4H_2O$ (97 mg, 0.39 mmol) in CH_3OH/H_2O (1 mL) added. A little triethylamine was added, and the reflux continued for 36 h. The reaction mixture was diluted with CH_2Cl_2 (20 mL), washed with water (20 mL), and dried ($MgSO_4$), and solvent was removed under reduced pressure. Flash column chromatography (silica, 1:1 CH_2Cl_2/hexane) followed by recrystallization from CH_2Cl_2/CH_3OH gave **6**·Ni as a red-purple solid (25 mg, 71%). ^{1}H-NMR ($CDCl_3$, 270 MHz): δ 7.02 (d, 1H, ^3J = 15.9 Hz, $H_{ethenyl}$), 7.15 (d, 1H, ^3J = 15.9 Hz, $H_{ethenyl}$), 7.29 (d, 2H, ^3J = 8.2 Hz, H_{Ar}), 7.65−7.78 (m, 12H, $H_{m,pPh}$), 7.80 (d, 2H, ^3J = 8.1 Hz, H_{Ar}), 7.97−8.07 (m,

8H, H_{oPh}), 8.69−8.75 (m, 6H, $H_{pyrrole}$), 8.94 (s, 1H, $H_{pyrrole}$), 9.99 (s, 1H, CHO). UV−vis (CH_2Cl_2): λ_{max} (log ϵ) 430 (5.24), 541 (4.22), 579 (4.10). HRMS, *m*/*z*: calcd for MH^+ ($C_{53}H_{35}N_4O^{58}Ni$), 801.2164; found, 801.2164.

6·Pd. Aldehyde **6** (10 mg, 13 μmol) was refluxed in toluene (5 mL), and $PdCl_2(NCPh)_2$ (11 mg, 29 μmol) was added. After 30 min of refluxing, TLC showed no further change, so the solvent was removed under pressure and the resulting black material flash column chromatographed (silica, 3:2 CH_2Cl_2/hexane). The first bright red fraction was collected, the solvent was removed under reduced pressure, and the solid was recrystallized from CH_2Cl_2/CH_3OH to give **6**·Pd (10 mg, 91%) as a red-purple powder. ^{1}H-NMR (270 MHz, $CDCl_3$): δ 7.11 (d, 1H, ^3J = 15.9 Hz, $H_{ethenyl}$), 7.22 (d, 1H, ^3J = 15.9 Hz, $H_{ethenyl}$), 7.33 (d, 2H, ^3J = 8.2 Hz, H_{Ar}), 7.68−7.84 (m, 14H, $H_{m,pPh}$ and H_{Ar}), 8.10−8.21 (m, 8H, Hz, H_{oPh}), 8.66−8.81 (m, 6H, $H_{pyrrole}$), 9.01 (m, 1H, $H_{pyrrole}$), 9.99 (s, 1H, CHO). UV−vis (CH_2Cl_2): λ_{max} (log ϵ) 426 (5.36), 533 (4.45), 569 (4.27) nm. HRMS, *m*/*z*: calcd for M^+ ($C_{53}H_{34}N_4O^{106}Pd$), 848.1767; found, 848.1752.

7·Ni. Aldehyde **7** (51 mg, 68 μmol) and $NiBr_2$ (36 mg, 0.16 mmol) were heated to reflux in DMF (5 mL). Almost immediately TLC indicated no starting material remained. The solvent was removed under high vacuum and the resulting material flash column chromatographed (silica, 1:1 CH_2Cl_2/hexane). Recrystallization from CH_2Cl_2/MeOH gave **7**·Ni (43 mg, 79%) as a purple solid. ^{1}H-NMR (270 MHz, $CDCl_3$): δ 6.96 (d, 1H, ^3J = 16.0 Hz, $H_{ethenyl}$), 7.17 (d, 1H, ^3J = 16.0 Hz, $H_{ethenyl}$), 7.44−7.49 (m, 2H, H_{Ar}), 7.64−7.80 (m, 14H, $H_{m,pPh}$ and H_{Ar}), 7.99−8.08 (m, 8H, H_{oPh}), 8.69−8.79 (m, 6H, $H_{pyrrole}$), 8.94 (s, 1H, $H_{pyrrole}$), 10.06 (s, 1H, CHO). UV−vis (CH_2Cl_2): λ_{max} (log ϵ) 425 (5.33), 538 (4.26), 574 (4.03) nm. HRMS, *m*/*z*: calcd for M^+ ($C_{53}H_{34}N_4O^{58}Ni$), 800.2086; found, 800.2129.

8·Ni. Aldehyde **8** (31 mg, 42 μmol) was refluxed in $CHCl_3$ (10 mL), and a slurry of $Ni(OAc)_2{\cdot}4H_2O$ (149 mg, 0.60 mmol) in CH_3OH/H_2O (1.5 mL/ 0.2 mL) was added. After 5 days, TLC indicated that no **8** remained, so the reaction mixture was diluted with CH_2Cl_2 (20 mL), washed with water (2 × 20 mL), and dried ($MgSO_4$), and solvent was removed under reduced pressure. Flash column chromatography (silica 1:1 CH_2Cl_2/hexane) followed by recrystallization from CH_2Cl_2/CH_3OH gave **8**·Ni (30 mg, 89%) as a red-purple solid. ^{1}H-NMR (270 MHz, $CDCl_3$): δ 6.86 (d, 1H, ^3J = 15.9 Hz, $H_{ethenyl}$), 7.11 (d, 1H, ^3J = 7.6 Hz, H_{Ar}), 7.34 (app t, 1H, ^3J = 7.6 Hz, H_{Ar}), 7.45 (app t, 1H, ^3J = 7.6 Hz, H_{Ar}), 7.58−7.74 (m, 12H, $H_{m,pPh}$), 7.79 (dd, 1H, ^3J = 7.6, ^4J = 1.2 Hz, H_{Ar}), 7.92−8.06 (m, 9H, H_{oPh} and $H_{ethenyl}$), 8.65−8.70 (m, 6H, $H_{pyrrole}$), 8.95 (s, 1H, $H_{pyrrole}$), 10.40 (s, 1H, CHO). UV−vis (CH_2Cl_2): λ_{max} (log ϵ) 427 (5.36), 539 (4.33), 576 (4.12) nm. HRMS, *m*/*z*: calcd for M^+ ($C_{53}H_{34}N_4O^{58}Ni$), 800.2086; found, 800.2030.

8·Pd. Aldehyde **8** (13 mg, 17 μmol) was refluxed in CH_2Cl_2 (10 mL) and $PdCl_2(NCPh)_2$ (29 mg, 76 μmol) added. After 16 h of refluxing, TLC showed no further change so the solvent was removed under pressure and the resulting black material flash column chromatographed (silica, 1:1 CH_2Cl_2/hexane). The first bright red fraction was collected, the solvent removed under reduced pressure, and the solid was recrystallized from CH_2Cl_2/CH_3OH to give **8**·Pd (10 mg, 69%) as a red-purple powder. ^{1}H-NMR (270 MHz, $CDCl_3$): δ 6.96 (d, 1H, ^3J = 15.9 Hz, $H_{ethenyl}$), 7.22 (d, 1H, ^3J = 7.9 Hz, H_{Ar}), 7.40 (app t, 1H, ^3J = 7.9 Hz, H_{Ar}), 7.52 (app t, 1H, ^3J = 7.9 Hz, H_{Ar}), 7.65−7.82 (m, 12H, $H_{m,pPh}$), 7.84 (d, 1H, ^3J = 7.9 Hz, H_{Ar}), 8.09 (d, 1H, ^3J = 15.9 Hz, $H_{ethenyl}$), 8.10−8.22 (m, 8H, H_{oPh}), 8.66 (d, 1H, ^3J = 4.9 Hz, $H_{pyrrole}$), 8.74 (d, 1H, ^3J = 4.9 Hz, $H_{pyrrole}$), 8.76−8.81 (m, 4H, $H_{pyrrole}$), 9.04 (s, 1H, $H_{pyrrole}$), 10.41 (s, 1H, CHO). UV−vis (CH_2Cl_2): λ_{max} 424, 531, 567 nm. HRMS, *m*/*z*: calcd for M^+ ($C_{53}H_{34}N_4O^{106}Pd$), 848.1767; found, 848.1777.

Acknowledgment. We are grateful for support of this work from The Public Good Science Fund (MAU602), the Massey University Research Fund, the Massey University Postgraduate Scholarship and Graduate Research Fund, the William Georgetti Scholarship, and the Young Scientists' Fund, Royal Society of New Zealand (D.C.W.R.). Support from the New Zealand Lottery Commission and the University of Otago Research Committee is gratefully acknowledged and support in part from The Public Good Science Fund (UOO-508). We also thank the University of Otago Chemistry Department for the award of a Ph.D. scholarship to P.A.C.

Supporting Information Available: Figures showing the electronic spectral changes of **2**−**5**, **9**, **10**, **2**·Ni, and **4**·Ni and RR spectra of **3** (9 pages). Ordering information is given on any current masthead page.

IC9702330